

## Hole-Transporting Periodic Mesoporous Organosilica

Norihiro Mizoshita, Masamichi Ikai, Takao Tani, and Shinji Inagaki\*

Toyota Central R&D Laboratories, Inc., Nagakute, Aichi 480-1192, Japan, and Core Research for Evolutional Science and Technology (CREST), Japan Science and Technology Agency (JST), Kawaguchi, Saitama 332-0012, Japan

Received June 18, 2009; E-mail: inagaki@mosk.tytlabs.co.jp

Periodic mesoporous organosilicas (PMOs)<sup>1–3</sup> are attracting increasing attention due to their highly functional framework structures. Various organic bridging groups (R) ranging from aliphatic and aromatic hydrocarbons to heterocyclics and metal complexes can be densely and covalently embedded within the framework of mesoporous materials by surfactant-templated polycondensation of well-designed organosilane precursors (R[Si(OR')]<sub>n</sub>, n ≥ 2).<sup>2,3</sup> Since PMOs possess large surface areas, designable hybrid frameworks, and mesoscale periodic porous structures such as channel arrays and 3D cages, they have great potential for numerous applications, including optical<sup>4</sup> and catalytic systems.<sup>5</sup> A number of PMOs with aromatic and  $\pi$ -conjugated bridging groups have been developed,<sup>3</sup> and these PMOs have been shown to have useful optical properties, such as strong light absorption, fluorescence, and light harvesting and excitation energy transfer.<sup>3,4</sup> However, there has been no report on charge conduction in the frameworks of PMOs although other approaches to the development of charge-conductive porous materials have been proposed using inorganic semiconductors and metals.<sup>6</sup>

The goal of the present study is to achieve charge transport in the pore walls of mesoporous organosilica hybrids with the aid of electroactive organic bridges. Some nonstructured organosilica hybrids have been demonstrated to exhibit charge-transporting properties even in the presence of siloxane networks,<sup>7</sup> indicating the possibility of realizing charge-transporting PMOs. Periodic mesoporous organosilicas with charge-transporting frameworks may lead to the development of a new class of photovoltaic materials and photocatalytic systems involving electron-transfer processes. In particular, highly efficient electronic devices may be fabricated if efficient generation and conduction of charge carriers can be achieved in PMOs by forming p–n junctions with large surface areas at the framework–mesopore interface.<sup>8</sup>

One of the challenges in realizing charge-transporting PMOs is the formation of well-defined mesostructures from 100% electroactive organosilane precursors with large  $\pi$ -conjugates. Generally, synthesizing PMOs from 100% organosilane precursors containing bulky organic groups is difficult. This is attributable to the weak surfactant–precursor interactions resulting from the low density of polar silanol groups separated by bulky organic groups. Recently, we reported the synthesis of visible-light-absorptive mesoporous films from bulky oligo(phenylenevinylene) (OPV, –C<sub>6</sub>H<sub>4</sub>–C<sub>2</sub>H<sub>2</sub>–C<sub>6</sub>H<sub>2</sub>R'<sub>2</sub>–C<sub>2</sub>H<sub>2</sub>–C<sub>6</sub>H<sub>4</sub>–) rod-like organosilane precursors.<sup>31</sup> However, a large amount of pure silica precursor (tetraethoxysilane, >50 wt %) was required to be mixed with the OPV precursors to obtain ordered mesoporous OPV films. The small ratio of the hydrophilic silyl groups to the hydrophobic OPV moieties would suppress interactions between hydrolyzed OPV precursors and surfactant micelles, resulting in the formation of nonordered OPV materials from 100% OPV precursors. Proper molecular design of precursors is required to

achieve both the formation of periodic mesostructures and charge transport in the organosilica pore walls.

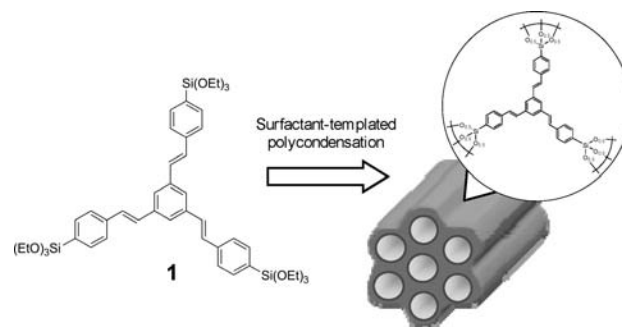


**Figure 1.** Preparation of mesoporous phenylenevinylene–silica hybrids from three-armed precursor **1**.

In the present paper, we first report long-range hole transport in the framework of mesoporous organosilica. For the preparation of mesoporous materials comprising a hole-transporting organosilica framework (Figure 1), we designed a three-armed phenylenevinylene compound with three triethoxysilyl groups (**1**), based on the strategies of (i) increasing the interaction between the precursor and the surfactant micelles; (ii) efficient formation of siloxane cross-links, resulting in stabilization of periodic mesoporous frameworks; and (iii) induction of charge hopping between organic bridges due to dense accumulation of the two-dimensionally expanded  $\pi$ -system directly connected to the silica backbone. In the present study, mesoporous and electroactive organosilica hybrid films were prepared on quartz substrates by evaporation-induced self-assembly of nonionic template surfactant Brij76 (C<sub>18</sub>H<sub>37</sub>(OCH<sub>2</sub>CH<sub>2</sub>)<sub>10</sub>OH) and **1** without other pure silica precursors. The hole-transporting behavior in the mesoporous organosilica framework was examined by time-of-flight (TOF) measurements.

Organosilane precursor **1** was easily and efficiently synthesized by similar synthetic procedures to those used for rod-like OPV precursors.<sup>31</sup> A three-armed aromatic iodide, 1,3,5-tris(4-iodostyryl)benzene, was obtained from 1,3,5-tris(bromomethyl)benzene and 4-iodobenzaldehyde in two steps (81% yield). Rh-catalyzed silylation of 1,3,5-tris(4-iodostyryl)benzene afforded organosilane precursor **1** in 89% yield.

Mesoporous organosilica films were successfully obtained by acidic sol–gel polycondensation of **1** in the presence of template surfactant Brij76. Evaporation of solvents (THF and ethanol) from sol mixtures containing **1**, Brij76, and a catalytic amount of hydrochloric acid yielded transparent organosilica films (denoted as **1-Brij76-F**). Figure 2 shows the X-ray diffraction pattern of the organosilica film (solid line). The film showed an intense diffraction peak at  $d = 5.26$  nm corresponding to the formation of a periodic mesostructure. Weak diffraction peaks were also observed at  $d = 3.05$ , 2.63, 2.01, and 1.72 nm. The reciprocals of the  $d$ -spacing

values are in the ratio of  $1:\sqrt{3}:2:\sqrt{7}:3$ , which is typical of a hexagonal arrangement of mesochannels. After extraction of the template,<sup>9</sup> the periodic mesostructure of the organosilica hybrid was retained, although X-ray diffraction peaks were broadened and the main  $d$ -spacing value decreased to 4.91 nm (Figure 2, broken line). For the samples both before and after extraction of Brij76, no sharp peaks in X-ray diffraction were observed at a wide angle region ( $2\theta > 10^\circ$ ), indicating the absence of molecular-scale periodicity in the framework. Note that mesostructured organosilica films were obtained from 100% organosilane precursor **1** without adding other alkoxy silane precursors. The three-armed geometry of the precursor is effective for enhancing the interaction with the surfactant micelles and the formation of three-dimensional siloxane cross-links. Although direct observation of the mesoscale morphologies of **1-Brij76-F** by electron microscopy was difficult due to the collapse of the mesostructure by electron beam irradiation, the films likely possess mesochannel arrays that are similar to a hexagonal packing.

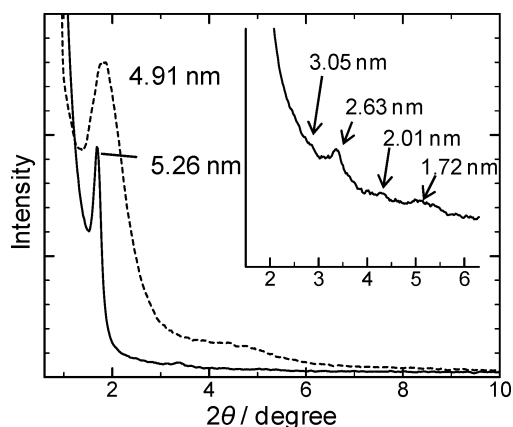


**Figure 2.** X-ray diffraction patterns of **1-Brij76-F** before (solid line) and after (broken line) extraction of Brij76.

The porosity of the extracted sample was examined by nitrogen adsorption–desorption isotherm measurements (see Supporting Information). The isotherm was classified as type I (micropore) rather than type IV (mesopore), likely due to the shrinkage of the periodic mesopores indicated by the X-ray diffraction measurements. However, the DFT pore diameter was calculated to be 2.4 nm, indicating small mesopores. The Brunauer–Emmett–Teller (BET) surface area and pore volume were  $941 \text{ m}^2 \text{ g}^{-1}$  and  $0.41 \text{ cm}^3 \text{ g}^{-1}$ , respectively. The large surface area is thought to result from the formation of a surfactant-templated porous structure. Assuming a hexagonal channel array in the extracted material, the thickness of the pore wall is estimated to be  $\sim 3.3 \text{ nm}$ , suggesting that the pore wall consists of three or four layers of the nonaligned phenylenevinylene–silica repeating unit. The organosilica hybrid prepared from **1** is available as a porous host material made of the photo- and electroactive phenylenevinylene–silica framework with a large surface area.

The hole-transporting behavior of the mesostructured film **1-Brij76-F** was examined by TOF measurements. Under application of DC electric fields, photocurrent generation and dispersive charge transport were observed for **1-Brij76-F** upon laser pulse irradiation ( $\lambda = 337 \text{ nm}$ ) on the side of the positive electrode of the cells (Figure 3a), indicating conduction of photogenerated holes within the organosilica framework of the mesostructured **1-Brij76-F** film. Figure 3b shows the hole mobilities calculated using the transit times of the charge carriers as determined from double logarithmic plots of the transient photocurrent as a function of time. The hole mobility in **1-Brij76-F** was  $\sim 3.2 \times 10^{-5} \text{ cm}^2 \text{ V}^{-1} \text{ s}^{-1}$  at an electric field strength of 0.6 MV

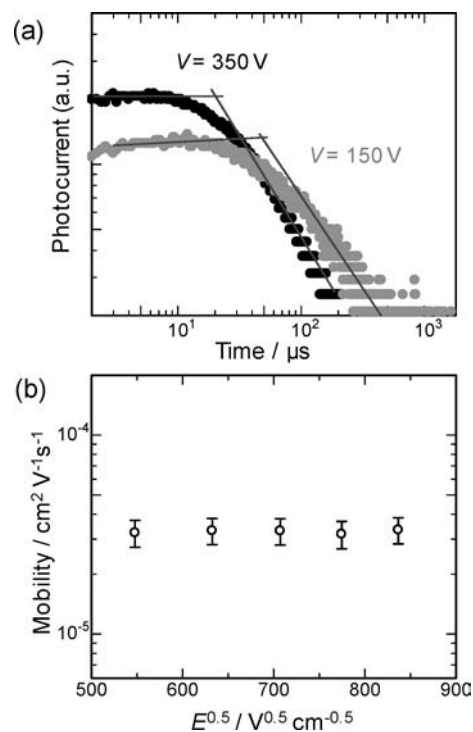


**Figure 3.** (a) Double logarithmic plots of transient photocurrent of **1-Brij76-F** (thickness:  $5 \mu\text{m}$ ) as a function of time at applied voltages of 150 and 350 V. (b) Plot of the hole mobility of **1-Brij76-F** versus electric field strength.

$\text{cm}^{-1}$ . The dependence of the hole mobility on the electric field strength was not clearly observed in the present range of measurements (Figure 3b). On the other hand, the hole mobilities in amorphous films of poly(*p*-phenylenevinylene) polymers<sup>10</sup> have been reported to be on the order of  $10^{-5} \text{ cm}^2 \text{ V}^{-1} \text{ s}^{-1}$ . The hole-transporting properties of the mesostructured phenylenevinylene–silica hybrid are comparable to those of  $\pi$ -conjugated organic amorphous polymers. The hole-transporting behavior of a nonstructured homopolymer film prepared from **1** (denoted as **1-F**) and neat precursor **1** (polycrystalline solid) was measured as a reference sample. Nonstructured organosilica film **1-F** generated photocurrents, and the hole mobility was determined to be  $\sim 5.1 \times 10^{-5} \text{ cm}^2 \text{ V}^{-1} \text{ s}^{-1}$ , which is slightly higher than that of **1-Brij76-F**. This result indicates that hole conduction in the dense phenylenevinylene–silica network formed by polycondensation of **1** alone is not strongly hindered by the introduction of mesostructures. No photocurrent was observed for neat precursor **1**. Hole trapping in grain boundaries of the crystalline solids or poor contact between the sample and electrodes can persist in the polycrystalline material. Molecular packing of uncondensed **1** in the crystal lattice may also impede hole hopping between organic moieties.

Spectroscopic measurements of the organosilica films indicate that the three-armed phenylenevinylene bridges are densely embedded within the organosilica framework. Figure 4 shows UV–vis and fluorescence spectra of **1-Brij76-F**, **1-F**, neat precursor **1** (polycrystalline solid), and a dilute 2-propanol solution of **1**. Compared to the solution of **1**, organosilica films **1-Brij76-F** and **1-F** showed slight blue shifts of the absorption bands from 319 to 312 nm, suggesting partial  $\pi$ -stacking of phenylenevinylene bridges in the frameworks. The fluorescence spectra of the films showed red-shifted broad emissions that are attributable to the excimer band at 423 nm. These results indicate that phenylenevinylene bridges fixed within the frameworks are densely packed and interactive in the excited state. The arrangement of the phenylenevinylene units, which results from

the polycondensation of **1** alone, should facilitate charge hopping between the organic bridging groups, leading to photocurrent generation observed using the TOF method. In contrast, an absorption band of the polycrystalline solid of **1** exhibited a red shift in the UV-vis spectrum, and the fluorescence spectrum was similar to that of the 2-propanol solution of **1**. In the crystal consisting of the uncondensed precursor, the  $\pi$ -conjugation length of the precursor molecule may be extended due to the increased planarity, whereas intermolecular interactions and parallel  $\pi$ -stacking appear to be suppressed in the crystal lattice, which may be the reason for the lack of charge conduction.

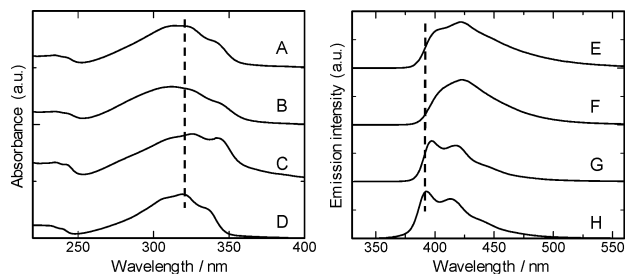


**Figure 4.** UV-vis (left) and fluorescence spectra (right, excited at  $\lambda = 320$  nm) of the organosilica and organosilane materials: (A, E) **1-Brij76-F**; (B, F) **1-F**; (C, G) neat precursor **1** (polycrystalline solid); (D, H) 2-propanol solution of **1** ( $5 \times 10^{-6}$  M).

In conclusion, mesostructured organosilica hybrids with electroactive phenylenevinylene bridges were successfully obtained by surfactant-templated polycondensation of a three-armed organosilane precursor. Hole transport in the pore walls of the mesostructured organosilica was achieved, and the hole mobilities were on the order of  $10^{-5} \text{ cm}^2 \text{ V}^{-1} \text{ s}^{-1}$ . The present results broaden the potential application of mesostructured organosilica materials in novel photocatalytic and photovoltaic systems, where the mesoporous structure with large surface and interfacial areas is greatly advantageous to promote the transfer of mass, charge, and energy in the mesopores or at the framework-mesopore interface. In the future, we hope to increase the hole mobilities in the pore walls by enhancing the molecular-scale ordering of the densely embedded  $\pi$ -conjugated bridges, because well-stacked OPV molecules are reported to exhibit quite high carrier mobilities on the order of  $10^{-1} \text{ cm}^2 \text{ V}^{-1} \text{ s}^{-1}$  in organic field effect transistors.<sup>11</sup>

**Supporting Information Available:** Complete ref 10a, experimental details, and additional data on infrared spectra, nitrogen adsorption-desorption isotherm, transient photocurrents, X-ray diffraction, solid state NMR, and TGA analysis. This material is available free of charge via the Internet at <http://pubs.acs.org>.

## References

- (1) (a) Hunks, W. A.; Ozin, G. A. *J. Mater. Chem.* **2005**, *15*, 3716–3724. (b) Hoffmann, F.; Cornelius, M.; Morell, J.; Fröba, M. *Angew. Chem., Int. Ed.* **2006**, *45*, 3216–3251. (c) Fujita, S.; Inagaki, S. *Chem. Mater.* **2008**,

- 20, 891–908. (d) Nicole, L.; Boissière, C.; Grosso, D.; Quach, A.; Sanchez, C. *J. Mater. Chem.* **2005**, *15*, 3598–3627.
- (2) (a) Inagaki, S.; Guan, S.; Fukushima, Y.; Ohsuna, T.; Terasaki, O. *J. Am. Chem. Soc.* **1999**, *121*, 9611–9614. (b) Melde, B. J.; Holland, B. T.; Blanford, C. F.; Stein, A. *Chem. Mater.* **1999**, *11*, 3302–3308. (c) Asefa, T.; MacLachlan, M. J.; Coombs, N.; Ozin, G. A. *Nature* **1999**, *402*, 867–871. (d) Yoshina-Ishii, C.; Asefa, T.; Coombs, N.; MacLachlan, M. J.; Ozin, G. A. *Chem. Commun.* **1999**, 2539–2540. (e) Inagaki, S.; Guan, S.; Ohsuna, T.; Terasaki, O. *Nature* **2002**, *416*, 304–307. (f) Kuroki, M.; Asefa, T.; Whittall, W.; Kruk, M.; Yoshina-Ishii, C.; Jaroniec, M.; Ozin, G. A. *J. Am. Chem. Soc.* **2002**, *124*, 13886–13895. (g) Kapoor, M. P.; Yang, Q.; Inagaki, S. *J. Am. Chem. Soc.* **2002**, *124*, 15176–15177. (h) Sayari, A.; Wang, W. *J. Am. Chem. Soc.* **2005**, *127*, 12194–12195. (i) Cornelius, M.; Hoffmann, F.; Fröba, M. *Chem. Mater.* **2005**, *17*, 6674–6678. (j) Xia, Y.; Wang, W.; Mokaya, R. *J. Am. Chem. Soc.* **2005**, *127*, 790–798. (k) Olkhovoyk, O.; Jaroniec, M. *J. Am. Chem. Soc.* **2005**, *127*, 60–61.
- (3) (a) Peng, H.; Tang, J.; Yang, L.; Pang, J.; Ashbaugh, H. S.; Brinker, C. J.; Yang, Z.; Lu, Y. *J. Am. Chem. Soc.* **2006**, *128*, 5304–5305. (b) Cornelius, M.; Hoffmann, F.; Ufer, B.; Behrens, P.; Fröba, M. *J. Mater. Chem.* **2008**, *18*, 2587–2592. (c) Minoofar, P. N.; Dunn, B. S.; Zink, J. I. *J. Am. Chem. Soc.* **2005**, *127*, 2656–2665. (d) Johansson, O.; Zink, J. I. *J. Am. Chem. Soc.* **2007**, *129*, 14437–14443. (e) Maegawa, Y.; Goto, Y.; Inagaki, S.; Shimada, T. *Tetrahedron Lett.* **2006**, *47*, 6957–6960. (f) Goto, Y.; Mizoshita, N.; Ohtani, O.; Okada, T.; Shimada, T.; Tani, T.; Inagaki, S. *Chem. Mater.* **2008**, *20*, 4495–4498. (g) Whittall, W.; Cademartiri, L.; Ozin, G. A. *J. Am. Chem. Soc.* **2007**, *129*, 15644–15649. (h) Mizoshita, N.; Goto, Y.; Kapoor, M. P.; Shimada, T.; Tani, T.; Inagaki, S. *Chem.–Eur. J.* **2009**, *15*, 219–226. (i) Mizoshita, N.; Goto, Y.; Tani, T.; Inagaki, S. *Adv. Funct. Mater.* **2008**, *18*, 3699–3705. (j) Wahab, M. A.; Sudhakar, S.; Teo, E.; Sellinger, A. *Chem. Mater.* **2008**, *20*, 1855–1861. (k) Nguyen, T. P.; Hesemann, P.; Gaveau, P.; Moreau, J. J. E. *J. Mater. Chem.* **2009**, *19*, 4164–4171.
- (4) (a) Tani, T.; Mizoshita, N.; Inagaki, S. *J. Mater. Chem.* **2009**, *19*, 4451–4456. (b) Inagaki, S.; Ohtani, O.; Goto, Y.; Okamoto, K.; Ikai, M.; Yamanaka, K.-i.; Tani, T.; Okada, T. *Angew. Chem., Int. Ed.* **2009**, *48*, 4042–4046.
- (5) Yang, Q.; Liu, J.; Zhang, L.; Li, C. *J. Mater. Chem.* **2009**, *19*, 1945–1955.
- (6) (a) Schüth, F. *Chem. Mater.* **2001**, *13*, 3184–3195. (b) Yang, P.; Zhao, D.; Margolese, D. I.; Chmelka, B. F.; Stucky, G. D. *Chem. Mater.* **1999**, *11*, 2813–2826. (c) Yamauchi, Y.; Takai, A.; Komatsu, M.; Sawada, M.; Ohsuna, T.; Kuroda, K. *Chem. Mater.* **2008**, *20*, 1004–1011. (d) Neyshadt, S.; Kalina, M.; Frey, G. L. *Adv. Mater.* **2008**, *20*, 2541–2546. (e) Aprile, C.; Teruel, L.; Alvaro, M.; Garcia, H. *J. Am. Chem. Soc.* **2009**, *131*, 1342–1343. (f) Kong, L.; Chen, H.; Hua, W.; Zhang, S.; Chen, J. *Chem. Commun.* **2008**, 4977–4979. (g) Li, X.; Bian, Z.; Zhu, J.; Huo, Y.; Li, H.; Lu, Y. *J. Am. Chem. Soc.* **2007**, *129*, 4538–4539. (h) Armatas, G. S.; Kanatzidis, M. G. *Nature* **2006**, *441*, 1122–1125. (i) Warren, S. C.; Messina, L. C.; Slaughter, L. S.; Kamperman, M.; Zhou, Q.; Gruner, S. M.; DiSalvo, F. J.; Wiesner, U. *Science* **2008**, *320*, 1748–1752. (j) Snaith, H. J.; Grätzel, M. *Adv. Mater.* **2007**, *19*, 3643–3647.
- (7) (a) Corriu, R. J. P.; Moreau, J. J. E.; Thepot, P.; Man, M. W. C.; Chorro, C.; Lère-Porte, J.-P.; Sauvajol, J.-L. *Chem. Mater.* **1994**, *6*, 640–649. (b) de Morais, T. D.; Chaput, F.; Boilot, J.-P.; Lahli, K.; Darracq, B.; Lévy, Y. *Adv. Mater. Opt. Electron.* **2000**, *10*, 69–79. (c) Dautel, O. J.; Wantz, G.; Almairac, R.; Flot, D.; Hirsch, L.; Lère-Porte, J.-P.; Pameix, J.-P.; Serein-Spirau, F.; Vignau, L.; Moreau, J. J. E. *J. Am. Chem. Soc.* **2006**, *128*, 4892–4901. (d) Peng, H.; Lu, Y. *Adv. Mater.* **2008**, *20*, 797–800. (e) Yang, L.; Peng, H.; Huang, K.; Mague, J. T.; Li, H.; Lu, Y. *Adv. Funct. Mater.* **2008**, *18*, 1526–1535.
- (8) (a) Coakley, K. M.; McGehee, M. D. *Appl. Phys. Lett.* **2003**, *83*, 3380–3382. (b) Sun, B.; Marx, E.; Greenham, N. C. *Nano Lett.* **2003**, *3*, 961–963. (c) Ravirajan, P.; Haque, S. A.; Durrant, J. R.; Poplavskyy, D.; Bradley, D. D. C.; Nelson, J. J. *Appl. Phys.* **2004**, *95*, 1473–1480. (d) Yan, H.; Lee, P.; Armstrong, N. R.; Graham, A.; Evmenenko, G. A.; Dutta, P.; Marks, T. J. *J. Am. Chem. Soc.* **2005**, *127*, 3172–3183.
- (9) Extraction of the template was performed after exposure to vapor of ammonia aqueous solution. See Supporting Information.
- (10) (a) Huang, Y.-F.; et al. *Adv. Funct. Mater.* **2007**, *17*, 2902–2910. (b) Büttling, W.; Lebedev, E.; Karg, S.; Dittrich, T.; Petrova-Koch, V.; Schwörer, M. *Proc. SPIE* **1998**, *3281*, 257–265. (c) Gailberger, M.; Bässler, H. *Phys. Rev. B* **1991**, *44*, 8643–8651.
- (11) Yasuda, T.; Saito, M.; Nakamura, H.; Tsutsui, T. *Appl. Phys. Lett.* **2006**, *89*, 182108.

JA9050263